Spatial patterns and mechanisms of the quasi-biennial oscillation–annual beat of ozone

Xun Jiang,[1,2] Dylan B. A. Jones,[3] Runlie Shia,[1] Duane E. Waliser,[4] and Yuk L. Yung[1]

Received 7 April 2005; revised 19 July 2005; accepted 31 August 2005; published 13 December 2005.

[1] An idealized two-dimensional chemistry and transport model is used to investigate the spatial patterns of, and mechanism for, the quasi-biennial oscillation–annual beat (QBO-AB) signal in ozone in the tropics and subtropics. Principal component analysis is applied to the detrended, deseasonalized, and filtered total column ozone anomaly from the standard model. The first two empirical orthogonal functions (EOFs) capture over 98.5% of the total variance. The first EOF, accounting for 70.3% of the variance, displays a structure attributable to the approximately symmetric QBO with a period of 28 months. The second EOF, capturing 28.2% of the variance, is related to the QBO-AB around 20 months. An extended EOF analysis reveals the characteristic pattern of the downward propagation of QBO and upward propagation of QBO-AB. The model results are compared to those from the merged ozone data. Sensitivity experiments indicate that the QBO-AB is produced primarily as a result of the dynamical QBO-AB in the mean meridional circulation and by the interaction between the QBO and the annual cycle in transport, each contributing roughly equally to the forcing of QBO-AB. The interaction between the QBO in the transport fields and the annual cycle in chemistry plays a minor role.

Citation: Jiang, X., D. B. A. Jones, R. Shia, D. E. Waliser, and Y. L. Yung (2005), Spatial patterns and mechanisms of the quasi-biennial oscillation–annual beat of ozone, *J. Geophys. Res.*, *110*, D23308, doi:10.1029/2005JD006055.

1. Introduction

[2] The quasi-biennial oscillation (QBO) (see Table 1 for list of acronyms) is the dominant interannual variability in the tropical stratosphere. It is primarily an oscillation in zonal winds in the stratosphere between downward propagating easterly and westerly phases, with a period of 22–32 months [*Reed et al.*, 1961; *Veryard and Ebdon*, 1961] (see extensive review by *Baldwin et al.* [2001]. There have been numerous observational studies of the QBO in the zonal wind, temperature, and ozone [e.g., *Angell and Korshover*, 1970; *Oltmans and London*, 1982; *Hasebe*, 1983; *Zawodny and McCormick*, 1991; *Pawson and Fiorino*, 1998; *Randel et al.*, 1999]. The mechanism by which the QBO modulates the ozone abundance in the stratosphere is well known [*Plumb and Bell*, 1982; *Baldwin et al.*, 2001]. When the QBO is in the westerly (easterly) phase, there is anomalous descending (upwelling) motion in the tropical stratosphere and anomalous upwelling (descending) motion in the subtropical stratosphere. This results in more (less) ozone at the equator in the westerly (easterly) QBO phase [*Gray and Dunkerton*, 1990; *Tung and Yang*, 1994a; *Hasebe*, 1994; *Randel and Cobb*, 1994]. The QBO also induces large variations in ozone in the extratropical stratosphere through its modulation of the vertical propagation of planetary Rossby waves [*Holton and Tan*, 1980; *Dunkerton and Baldwin*, 1991] and through the QBO-induced meridional circulation (QBO-MMC) [*Kinnersley and Tung*, 1999; *Ruzmaikin et al.*, 2005].

[3] An outstanding deficiency in our understanding of the QBO in ozone is associated with the mechanism responsible for the QBO-related harmonics that have been detected in stratospheric ozone. Consider a multiplicative model

$$(1 + a\sin\omega_A t)(1 + b\sin\omega_Q t) = 1 + a\sin\omega_A t + b\sin\omega_Q t + ab(\sin\omega_A t)(\sin\omega_Q t),$$

where ω_A and ω_Q are the frequencies of the annual cycle and the QBO. The nonlinear term produces the sum and difference frequencies through the trigonometric identity

$$(\sin\omega_A t)(\sin\omega_Q t) = \frac{1}{2}\cos(\omega_A - \omega_Q)t - \frac{1}{2}\cos(\omega_A + \omega_Q)t.$$

As a result, the QBO and annual cycles will produce beat frequencies with periods of approximately 20 and 8.6 months, which was first found in the total column ozone data obtained by TOMS in the tropics and extratropics [*Tung and Yang*, 1994a, 1994b]. These frequencies have also been observed in the power spectra of angular

[1]Division of Geological and Planetary Sciences, California Institute of Technology, Pasadena, California, USA.
[2]Department of Environmental Science and Engineering, California Institute of Technology, Pasadena, California, USA.
[3]Department of Physics, University of Toronto, Toronto, Ontario, Canada.
[4]Sciences Division, Jet Propulsion Laboratory, California Institute of Technology, Pasadena, California, USA.

0148-0227/05/2005JD006055

Table 1. List of Acronyms

	Definition
2-D	two-dimensional
3-D	three-dimensional
BDC	Brewer-Dobson circulation
CTM	chemistry and transport model
DU	Dobson unit
EEOF	extended empirical orthogonal function
EOF	empirical orthogonal function
MMC	mean meridional circulation
MOD	merged ozone data
PCA	principal component analysis
QBO	quasi-biennial oscillation
QBO-AB	QBO-annual beat, around 20 months
QBO-AB′	QBO-annual beat, around 8 months
QBO-MMC	QBO-induced meridional circulation
VMR	volume-mixing ratio
ω_A	frequency of the annual cycle
ω_Q	frequency of QBO

momentum and planetary Rossby wave forcing in the stratosphere [*Baldwin and Tung*, 1994]. Using version 7 merged ozone data (MOD), *Camp et al.* [2003] carried out a principal component analysis (PCA) of the temporal and spatial patterns of the interannual variability of the total column ozone in the tropics from 1979 to 2002. They found that the first four empirical orthogonal functions (EOFs) captured over 93% of the variance of the detrended and deseasonalized data on interannual timescales. The PC associated with the third EOF (which accounted for 15% of the variance) had a dominant peak around 20 months (referred to as the QBO-annual beat (QBO-AB) hereinafter). The spatial pattern is a zonally symmetric, north-south tilted plane centered at the equator. A weaker signal at about 8 months (QBO-AB′ hereinafter) was also found in MOD. At present, a mechanistic understanding of the origin of these harmonics is still lacking. Such an understanding is critical to accurately account for the large QBO-induced interannual variability in ozone when trying to quantify the impact of human activity on ozone in the stratosphere.

[4] Using a two-dimensional (2-D) model, *Jones et al.* [1998] successfully reproduced the QBO beat frequencies in stratospheric ozone. They did not, however, perform a detailed analysis of the mechanism responsible for the beat in the model. More recently, *Jiang et al.* [2004] were able to simulate the QBO and the QBO-AB signals in column ozone from 1979 to 2002 using a 2-D chemical transport model (CTM) driven by transport fields derived from the National Centers for Environmental Prediction (NCEP) – Department of Energy Reanalysis 2. Here we extend the analysis of *Jiang et al.* [2004], using the 2-D model of *Jones* [1998] and *Jones et al.* [1998], to investigate the spatial pattern (latitude-altitude) of, and the mechanism for, the QBO-AB of ozone in the stratosphere. The reason for using the Jones model is as follows. The QBO signal given by *Jiang et al.* [2004] has a broad power spectrum, making it difficult to isolate the QBO from the QBO-AB. The situation will improve with a longer record. In the model of *Jones* [1998] and *Jones et al.* [1998] the parameterized QBO forcing produces an oscillation with a fixed period of ~28 months. There are no other sources of interannual variability in this idealized model. It is therefore a better tool to determine the mechanisms for producing the QBO-AB in ozone. The model of *Jones* [1998] and *Jones et al.* [1998], however, does not account for the QBO modulation of planetary wave breaking, which is responsible for the QBO in ozone in the extratropical stratosphere. We therefore focus here on understanding the mechanism responsible for the QBO-AB in ozone in the tropical and subtropical stratosphere.

[5] There are three possible mechanisms for the QBO-AB signal in column ozone. In the chemical tracer continuity equation, the interaction between the QBO and the annual cycle in the Brewer-Dobson circulation (BDC) and in the photochemical sources and sinks will both contribute to the QBO-AB [*Gray and Dunkerton*, 1990]. In addition, the mean meridional circulation (MMC) will possess a QBO-AB signal as a result of the interaction of the QBO and the annual cycle in the advection terms of the momentum equation in the tropics. This QBO-AB signal in the transport will also produce a QBO-AB signal in column ozone. However, it is unclear which is the predominant mechanism. We propose to test the different mechanisms through a series of sensitivity experiments listed in Table 2.

2. Modeling Ozone in the Tropics and Subtropics

2.1. Modeling Results

[6] The 2-D model is described in detail by *Jones et al.* [1998] and *Schneider et al.* [2000]. It has a horizontal resolution of 5° from pole-to-pole and a vertical resolution of 2 km from the surface to 80 km. It is a fully interactive primitive equation model in which the heating rates are calculated from model-derived ozone in the stratosphere. The model includes a comprehensive treatment of stratospheric chemistry. The effects of planetary wave breaking are specified as annually varying eddy diffusion coefficients K_{yy} based on *Newman et al.* [1986, 1988]. The QBO in zonal wind is reproduced in the model using mainly the parameterization of *Gray and Pyle* [1989] for the deposition of Kelvin and Rossby-gravity wave momentum in the tropical zonal wind. The Rossby-gravity wave dissipation is adopted from the formulation of *Holton and Lindzen* [1972].

[7] In the analysis presented here, we employ an offline version of the model, driven by the transport fields archived

Table 2. Description of Model Runs in Sensitivity Studies

Model Run	Description
Standard model	offline version of the 2-D model using the parameterized QBO circulation, annual cycle in the temperature field
Experiment A	only the QBO-AB signal kept in the transport fields, no annual cycle in the chemistry
Experiment B	only the annual cycle and QBO kept in the transport fields, no annual cycle in the chemistry
Experiment C	only the QBO signal kept in the transport fields, annual cycle in the chemistry

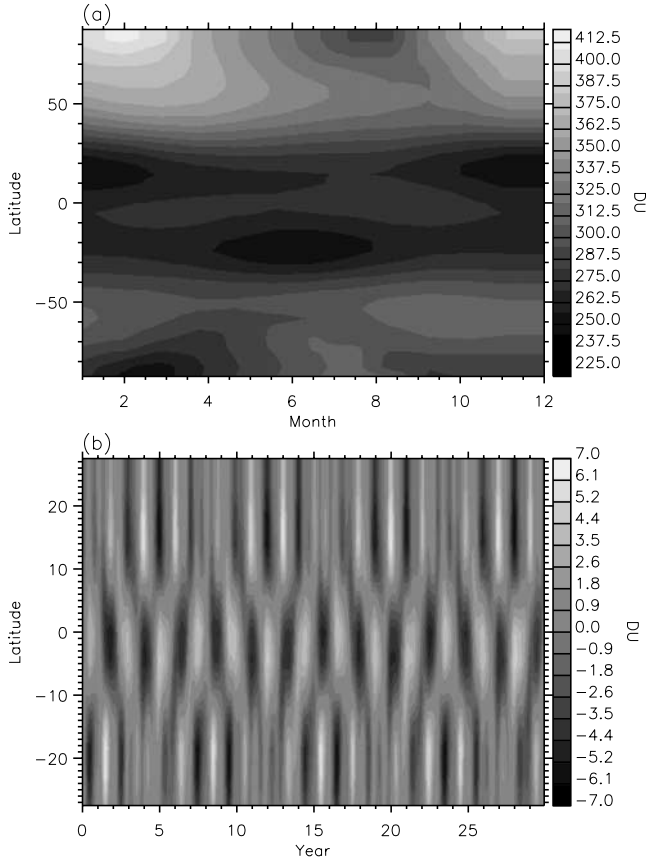

Figure 1. (a) Climatology and (b) anomaly of the total column ozone for the standard model. See color version of this figure at back of this issue.

from a 50-year simulation of the fully interactive model. The total column ozone climatology and the QBO ozone anomalies from 30 years simulation are shown in Figure 1. The annual cycle of the modeled ozone column abundance is consistent with observations. The QBO anomaly in ozone is calculated by removing the monthly mean annual cycle from the original total column ozone abundances. The model provides a good simulation of the QBO signal in the ozone columns. The amplitude of the ozone anomaly is ~7 Dobson units (DU). Estimates of the magnitude of the tropical anomaly range from about 6 DU by *Hasebe* [1983] to about 9 DU by *Zawodny and McCormick* [1991]. Using a least squares fit to the anomalies in column ozone, *Tung and Yang* [1994a] suggested that the amplitude of the QBO anomaly in middle and high latitudes is about 6 DU, about a quarter of the amplitude of the unfiltered anomaly.

[8] To investigate the magnitude of the QBO-AB and QBO-AB′, we apply band pass filters A and B to the column ozone from the 2-D CTM and MOD. The details of the band pass filters A and B, and other similarly constructed filters used in this study are presented in Table 3. Band pass filters A and B are desired to retain the signals of QBO-AB and QBO-AB′. Because the QBO-AB is not a strict oscillation around 20 months in the MOD and model, signal will be compensated through averaging over pure 20 months cycle. Thus the QBO-AB is averaged over 18 and 14 events for the model and MOD, respectively, when the QBO-AB signal reaches maximum at 17.5° N.

Table 3. Frequency Filters Used in the Models[a]

Filter	Period Windows, months	
	Passed	Blocked
Low pass A	(15, max)	(0, 12.5)
Band pass A	(18, 22.5)	(0, 17) and (24, max)
Band pass B	(7.7, 8.7)	(0, 7.3) and (9.1, max)
Band pass C	(15, 37)	(0, 12.5) and (50, max)
Band pass D	(11, 13)	(0,10.5) and (14, max)
Band pass E	(26.5, 33)	(0, 24) and (38, max)

[a]Passed ranges correspond to frequencies unaltered by the spectral window. Stopped ranges correspond to frequencies completely blocked. Frequencies in the transition intervals are damped; the spectral windows used are convolutions of a Hanning window and a step function. Max is 600 months.

Similar approach is applied to isolate the QBO-AB′ from the model and MOD. Mean QBO-AB and QBO-AB′ of 2-D CTM and MOD are shown in Figure 2. The magnitude of the QBO-AB in the 2-D CTM (solid line) is a little smaller than that in the MOD (dashed line). The magnitude of the QBO-AB′ in the model is similar to that in the MOD. The amplitude of the QBO-AB is about 2–3 times larger than that of the QBO-AB′ from the 2-D CTM and MOD. The reason will be given in section 3.1.

2.2. PCA of Ozone Column Abundance

[9] PCA is applied to the detrended, deseasonalized and filtered total column ozone anomaly from the 2-D CTM.

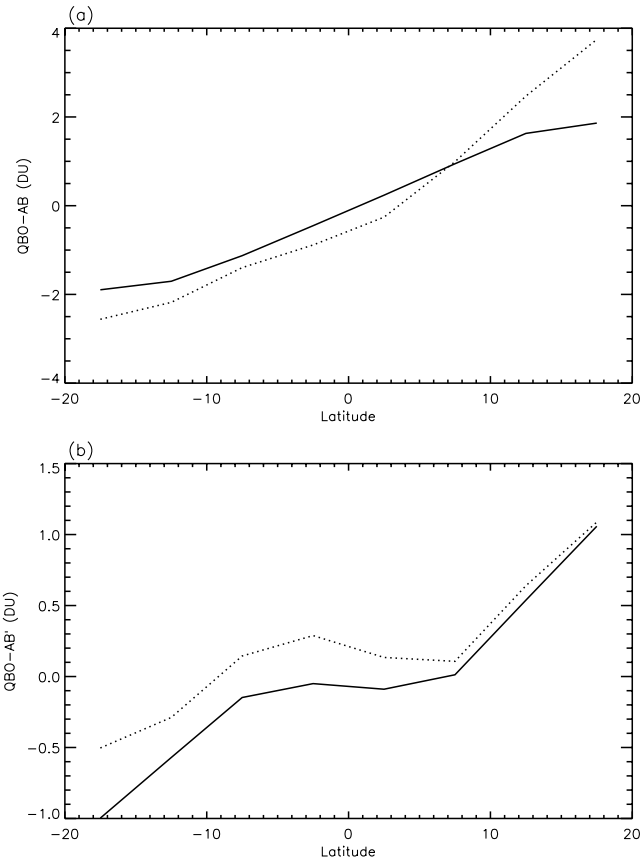

Figure 2. (a) Ozone QBO-AB and (b) QBO-AB′ signals from 2-D chemistry and transport model (CTM) (solid line) and merged ozone data (MOD) (dotted line).

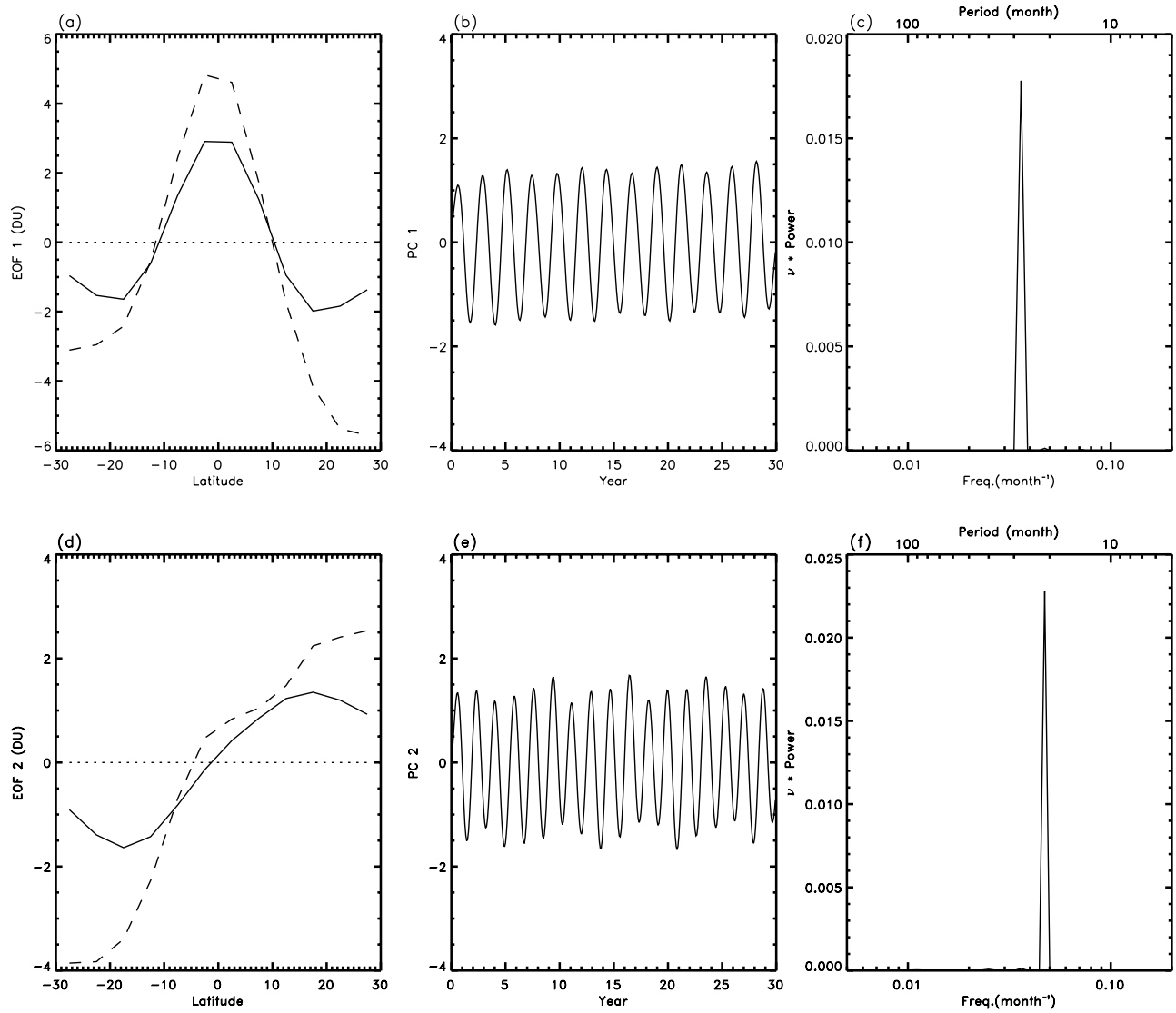

Figure 3. (left) Spatial empirical orthogonal function (EOF) patterns, (middle) principal component (PC) time series, and (right) spectra for the first two EOFs of the total column ozone from the standard model. The solid line represents the EOF patterns from the standard model. The dashed line represents the EOF patterns from the zonal mean MOD. Units of EOFs are Dobson units. (a) EOF_1, (b) PC_1, (c) spectrum for PC_1, (d) EOF_2, (e) PC_2, and (f) spectrum for PC_2.

Low-pass filter A is chosen to obtain a full signal from periods above 15 months and no signal from periods below 12.5 months. The first two EOFs capture 98.5% of the total variance of the filtered data, as shown in Figure 3. The fractions of variance for the leading EOFs are listed in Table 4. The first EOF captures 70.3% of the variance, and displays a structure similar to the QBO. It is approximately symmetric about the equator and oscillates about nodes at 10°N and 11°S. The values range from a high of 3 DU to a low of −2 DU. The magnitude of this mode is smaller than that of the first EOF pattern of the zonal mean MOD [*Jiang et al.*, 2004]. The associated principal component time series, PC1, is plotted in Figure 3b. The power spectral estimate of PC1, Figure 3c, shows a strong peak at 28 months. The phase of PC1 does not match the PC1 from the zonal mean MOD, because the observed QBO has a much broader spectral band around 28 months than that in

Table 4. Fractions of Variance Explained by EOFs

	EOF1, %	EOF2, %	EOF3, %	EOF4, %
PCA on the column O_3 from the standard model	70.3	28.2		
EEOF on the O_3 VMR from the standard model	24.3	23.6	16.1	15.6
EEOF on the band-pass-filtered O_3 VMR from MOD	23.4	21.8	9.5	8.4
PCA on the column O_3 from the experiment A	97.4			
PCA on the column O_3 from the experiment B	67.5	26.4		
PCA on the column O_3 from the experiment C	90.4	6.5	2	

the model. Ozone is transported to the polar region by the BDC. During the QBO westerly (easterly) phase, the BDC is weak (strong). Therefore the tropical total column ozone will increase (decrease), while the opposite will occur at higher latitudes.

[10] The second EOF, capturing 28.2% of the variance, oscillates about a node at the equator. Values range from 1.4 DU in the north to −1.6 DU in the south. It is similar to the third EOF pattern of the zonal mean MOD [*Jiang et al.*, 2004]; however, the magnitude is smaller than that in the zonal mean MOD. The power spectral estimate of the associated PC2 has a dominant peak around 20 months, suggesting that this EOF reflects the interaction of the annual cycle with the QBO signal.

2.3. Extended EOF Analysis of Ozone Mixing Ratio

[11] To study the interannual variability in the vertical distribution of ozone, particularly its spatial-temporal structure, we apply extended EOF (EEOF) [*Weare and Nasstrom*, 1982] to the deseasonalized ozone volume-mixing ratio (VMR) from the 2-D CTM. For this analysis, time is lagged −15 months to +14 months. The main advantage of EEOF analysis over PCA analysis in this case is that we can extract modes that exhibit systematic covariability in space and time, such as propagating "waves" [e.g., *Waliser et al.*, 2003]. Note that since EEOF modes are constrained in both space and time, the dominant modes typically do not capture as much overall variance as for a regular PCA. In this case, the first four EEOFs, shown in Figure 4, capture 79.6% of the total variance.

[12] The first two EEOFs capture 24.3% and 23.6% of the variance, respectively, and represent the QBO. Their spatial patterns and PCs are in quadrature. PC1 and PC2, plotted in Figures 4b and 4e, respectively, have maximum cross-correlation (= 0.98) at −7 months, which represents a complete period of about 28 months and is consistent with the power spectral estimate shown in Figures 4c and 4f. The third and fourth EEOF modes account for 16.1% and 15.6% of the variance, respectively, and correspond to the QBO-AB. Their spatial patterns and PCs are also in quadrature. PC3 and PC4, plotted in Figures 4h and 4k, have a maximum cross correlation (= 0.97) at 5 months. It is consistent with the power spectral estimates in Figures 4i and 4l, displaying a dominant period of about 20 months.

[13] To illustrate the propagation of the QBO and QBO-AB, respectively, we reconstruct the data using only the first two EEOF modes (i.e., $PC_1 \times EEOF_1 + PC_2 \times EEOF_2$), and then separately using only third and fourth EEOF modes (i.e., $PC_3 \times EEOF_3 + PC_4 \times EEOF_4$). Figure 5 shows these constructed data along the equator for the QBO mode, and at 12.5° N and 12.5° S for the QBO-AB mode. There is downward propagation of the ozone QBO as a result of the downward propagation of the dynamical QBO. In contrast, the ozone QBO-AB propagates upward. The ozone QBO-AB in 12.5° N has opposite sign to that in 12.5° S. The reason for the upward propagation of the QBO-AB will be given in section 3.1. The downward propagation speed of the QBO is about 0.6 km/month in the region of 20–36 km. The upward propagation speed of the QBO-AB is about 1.2 km/month in the region of 28–36 km. The downward propagation of the QBO in the ozone VMR is similar to that given by *Politowicz and Hitchman* [1997]. Using the diabatic-forcing method in their 2-D model, they also found that QBO in the deseasonalized and filtered ozone VMR propagates downward with a speed of 1 km/month in the region of 20–39 km. However, Politowicz and Hitchman did not find the QBO-AB.

2.4. Comparison With Observations

[14] To investigate the propagation characteristics of QBO and QBO-AB in the observed ozone data, we apply EEOF analysis to the deseasonalized, detrended, and filtered ozone VMR from version 8 MOD [*Wellemeyer et al.*, 2004]. Band-pass filter C is used to retain the QBO and QBO-AB signals. The first four EEOFs capture 63.1% of the total variance. The first EEOF, shown in Figure 6a, represents the QBO, accounting for 23.4% of the variance. The power spectral estimate of the PC1 shows a broad peak around 28 months. The spatial pattern of the first EEOF demonstrates that less (more) ozone is transported to the high latitudes in the westerly (easterly) phase of QBO. The second EEOF accounts for 21.8% of the variance and represents the QBO too. PC1 and PC2 have a maximum cross correlation (= 0.93) at 7 months. The third and fourth EEOFs, shown in Figures 6g and 6j, represent the asymmetric QBO-AB, accounting for 9.5% and 8.4% of the variance, respectively. PC1 and PC2 have a maximum cross correlation (= 0.92) at 5 months. The power spectra of PC3 and PC4 display dominant peak around 20 months. There is also small peak around QBO in the power spectra of PC3 and PC4.

[15] The propagations of the QBO and QBO-AB are shown in Figure 7. The downward propagation of the ozone QBO is similar to that in the model, although the propagation is weak in the lower stratosphere. This is because the QBO signal in the MOD has a broader spectral peak than that in the model, thus the signal is more complex. Unlike the idealized model, the length of the QBO phases in the MOD changes from year to year. We also find the upward propagation of the ozone QBO-AB in the MOD as in the model. The sign of the ozone QBO-AB is opposite in the different hemispheres. Because there is also QBO signal existed in the third and fourth modes, so the amplitude of the constructed signal from the third and fourth modes does not represent the real amplitude of the QBO-AB, which can explain why the amplitude is larger in the south than that in the north. The downward propagation speed of the QBO is about 1 km/month in the region of 32–43 km. The upward propagation speed of the QBO-AB is about 1.3 km/month in the same region.

[16] The spatial patterns of the first and second EEOFs in the model ozone VMR are similar to the first two modes

Figure 4. (left) Spatial extended EOF (EEOF) patterns, (middle) PC time series, and (right) spectra for the first four EEOFs at lag = 0 of the ozone volume-mixing ratio (VMR) from the standard model. Units of EEOFs are parts per million by volume (ppmv). (a, b, and c) $EEOF_1$, PC_1, and spectrum for PC_1. (d, e, and f) $EEOF_2$, PC_2, and spectrum for PC_2. (g, h, and i) $EEOF_3$, PC_3, and spectrum for PC_3. (j, k, and l) $EEOF_4$, PC_4, and spectrum for PC_4.

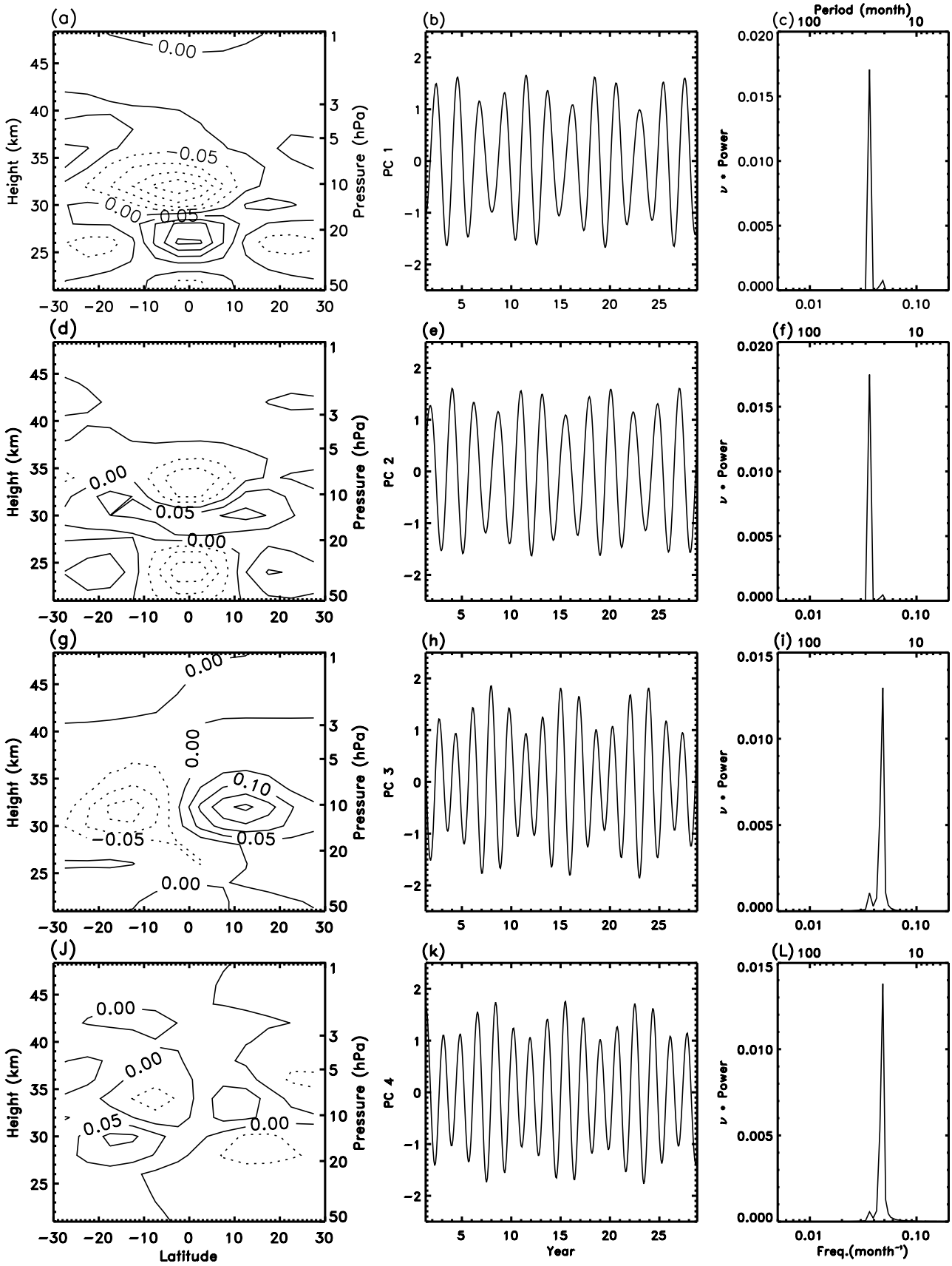
(a)
(b)
(c)
(d)
(e)
(f)
(g)
(h)
(i)
(J)
(k)
(L)
Height (km)
Pressure (hPa)
PC 1
PC 2
PC 3
PC 4
Period (month)
ν • Power
Latitude
Year
Freq.(month⁻¹)
0.00
−0.05
0.05
0.10

Figure 4

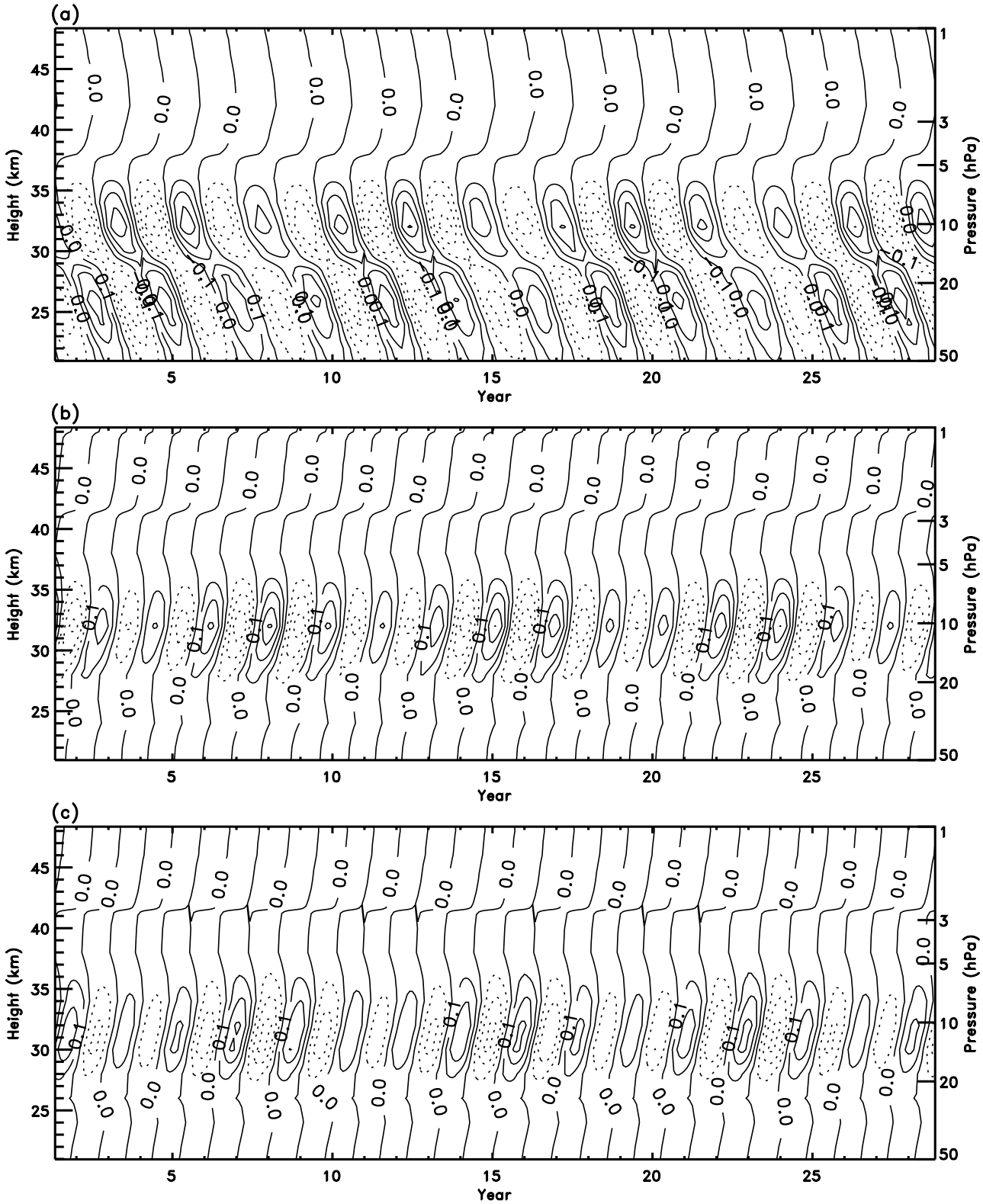

Figure 5. (a) $PC_1 \times EEOF_1 + PC_2 \times EEOF_2$ at equator, (b) $PC_3 \times EEOF_3 + PC_4 \times EEOF_4$ at 12.5° N, and (c) $PC_3 \times EEOF_3 + PC_4 \times EEOF_4$ at 12.5°S obtained at lag = 0 from the ozone VMR from the standard model. Units are ppmv.

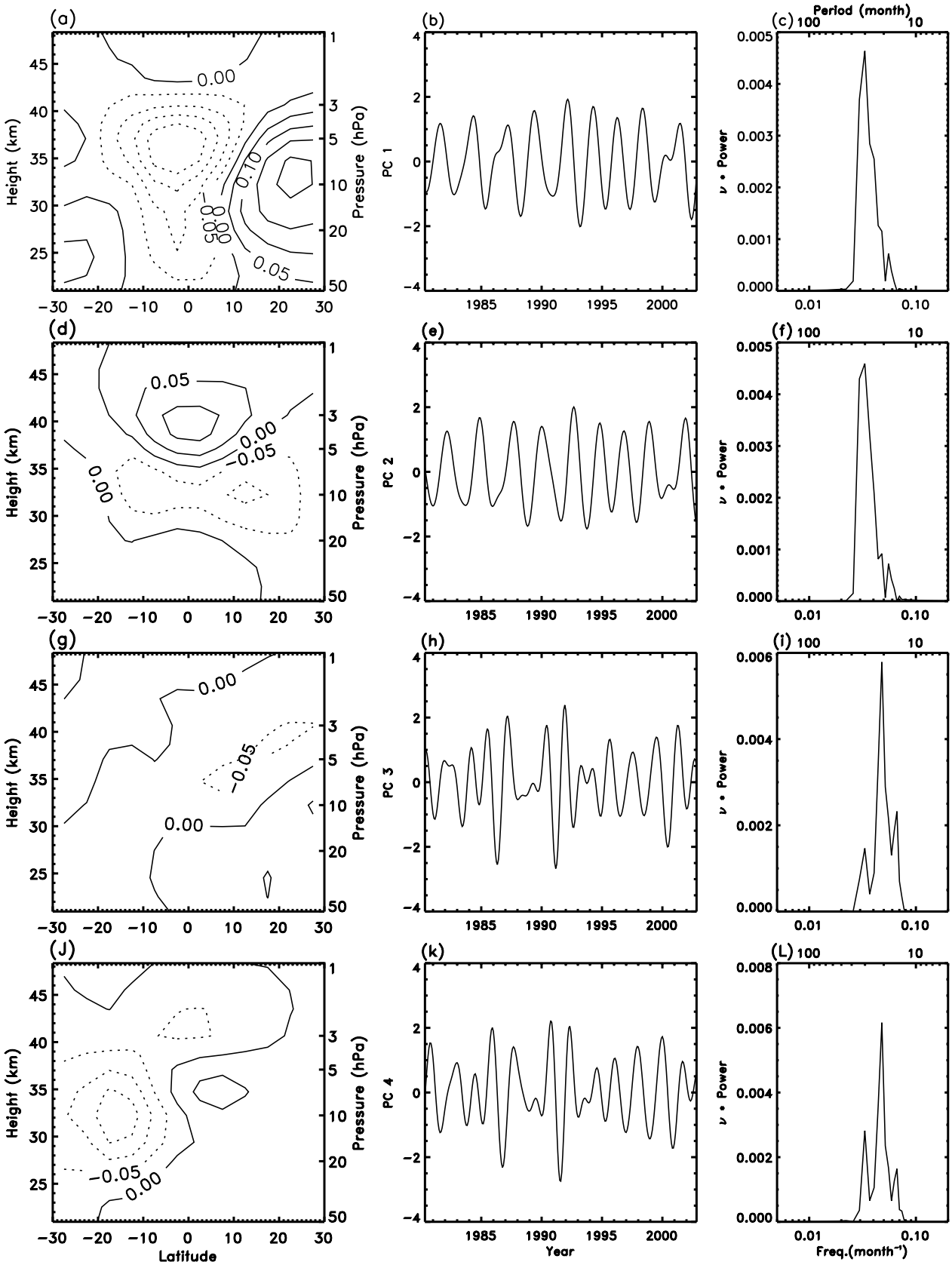

Figure 6. (left) Spatial EEOF patterns, (middle) PC time series, and (right) spectra for the first four EEOFs at lag = 0 of the band-pass-filtered ozone VMR from MOD. Units of EEOFs are ppmv. (a, b, and c) $EEOF_1$, PC_1, and spectrum for PC_1. (d, e, and f) $EEOF_2$, PC_2, and spectrum for PC_2. (g, h, and i) $EEOF_3$, PC_3, and spectrum for PC_3. (j, k, and l) $EEOF_4$, PC_4, and spectrum for PC_4.

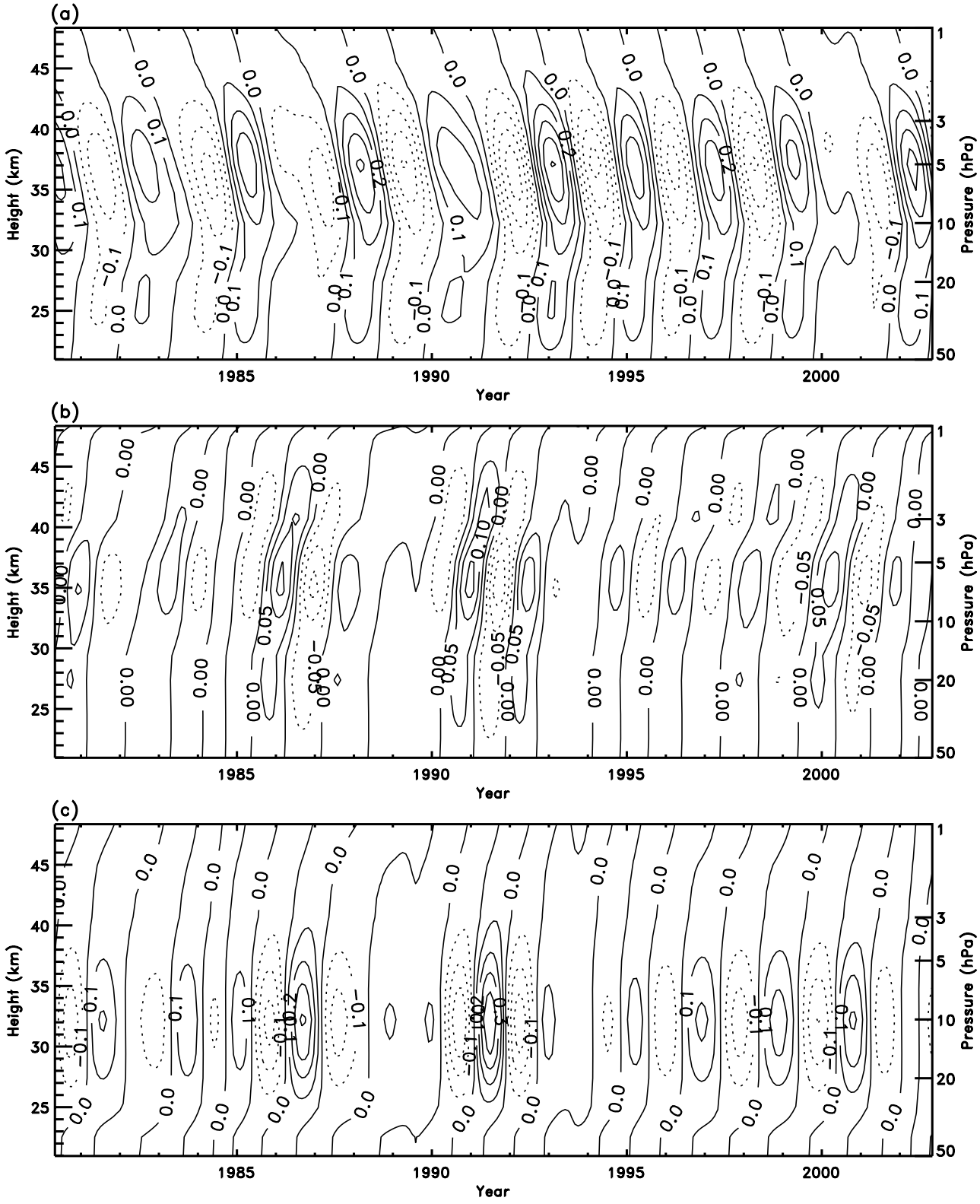

Figure 7. (a) $PC_1 \times EEOF_1 + PC_2 \times EEOF_2$ at equator, (b) $PC_3 \times EEOF_3 + PC_4 \times EEOF_4$ at 12.5°N, and (c) $PC_3 \times EEOF_3 + PC_4 \times EEOF_4$ at 12.5°S obtained at lag = 0 from the band-pass-filtered ozone VMR from MOD. Units are ppmv.

from singular-value decomposition (SVD) between the ozone VMR from SAGE II and the QBO zonal winds [*Randel and Wu*, 1996]. SVD for the two fields involves the covariance of two fields. As a result, the analysis of two fields by SVD will exhibit the highest temporal covariance between the two fields. Since the QBO is the dominant signal in the QBO zonal winds, they only find the QBO signal in ozone VMR. The QBO-AB was not found in their two-field SVD results.

3. Mechanisms for Generating QBO-AB

3.1. Theory of Harmonics

[17] We follow *Gray and Dunkerton* [1990] in the treatment of the interaction between the QBO and the annual cycle in column ozone. The continuity equation for the tracers in the model can be written as

$$\frac{\partial \chi}{\partial t} + \overline{v}\frac{\partial \chi}{\partial y} + \overline{w}\frac{\partial \chi}{\partial z} = (P - L) + \vec{\nabla} \cdot K\vec{\nabla}\chi \tag{1}$$

where χ is the mixing ratio, $\overline{v}$ and $\overline{w}$ are the mean meridional and vertical velocities, P and L represent photochemical production and loss rates, respectively, and K is the "eddy diffusion" coefficient, representing small-scale irreversible dispersions.

[18] Multiplying equation (1) by the density ρ and taking the vertical integral, we can approximately obtain

$$\frac{\partial C}{\partial t} + \overline{v}\frac{\partial C}{\partial y} = \int_0^\infty \rho(P - L)dz + \overline{\vec{\nabla} \cdot K\vec{\nabla}C} \tag{2}$$

where $C = \int_0^\infty \rho\chi dz$ is the column ozone. The nonlinear advection term, $\overline{v}\dfrac{\partial C}{\partial y}$, implies that the initial harmonics can interact to form new harmonics with frequencies equal to the sum or the difference of any pair of initial frequencies.

[19] We can explore the details of these harmonics by expanding the meridional velocity into its seasonal and QBO-dependent components

$$\overline{v} = v_0 + v_A \exp(i\omega_A t) + v_Q \exp(i\omega_Q t) + v_{AQ}^{+} \exp\left[i(\omega_A + \omega_Q)t\right] + v_{AQ}^{-} \exp\left[i(\omega_A - \omega_Q)t\right] \tag{3}$$

where the subscripts A and Q denote annual and quasi-biennial harmonics, v_A and v_Q are the amplitudes associated with the annual and quasi-biennial harmonics, v_{AQ}^{+} and v_{AQ}^{-} are the amplitudes associated with the sum and difference between the annual and quasi-biennial harmonics. Similarly, we can express the ozone column, C, as

$$C = C_0 + C_A \exp(i\omega_A t) + C_Q \exp(i\omega_Q t) + C_{AQ}^{+} \exp\left[i(\omega_A + \omega_Q)t\right] + C_{AQ}^{-} \exp\left[i(\omega_A - \omega_Q)t\right] + \ldots \tag{4}$$

where C_A and C_Q are the amplitudes associated with the annual and quasi-biennial oscillations for the column ozone, C_{AQ}^{+} and C_{AQ}^{-} are the amplitudes associated with the two beat frequencies. The photochemical production and loss rates can also be written as

$$(P - L) = (P - L)_0 + S_A \exp(i\omega_A t) \tag{5}$$

where S_A is the amplitude associated with the annual cycle of the photochemical production and loss rates.

[20] In the previous section, we found that the QBO-AB propagates upward and the amplitude of the QBO-AB is larger than that of QBO-AB′. Assuming the annual cycle signal does not propagate, the interaction between the annual cycle and the propagating QBO gives:

$$\sin(\omega_A t)\sin\left(\omega_Q t - \frac{\omega_Q}{W_Q}z\right) = \frac{1}{2}\left\{\cos\left[(\omega_A - \omega_Q)t + \frac{\omega_Q}{W_Q}z\right] - \cos\left[(\omega_A + \omega_Q)t - \frac{\omega_Q}{W_Q}z\right]\right\} \tag{6}$$

where W_Q is the phase speed of the QBO, t is time, and z is height. Thus the phase speeds of the QBO-AB and QBO-AB′ are separately

$$W_{AB} = -\frac{\omega_A - \omega_Q}{\omega_Q}W_Q \qquad W_{AB'} = \frac{\omega_A + \omega_Q}{\omega_Q}W_Q \tag{7}$$

Since the QBO propagates downward, $W_Q < 0$, the phase speed of the QBO-AB is positive (upward) and the phase speed of the QBO-AB′ is negative (downward).

[21] To investigate the ozone response to the QBO-AB and QBO-AB′ signals, we also need to consider the lifetime of O_3. Consider a heuristic model with pure sinusoidal forcing [*Camp et al.*, 2001]:

$$\frac{dy(t)}{dt} = -\frac{y(t)}{\tau} - \frac{F(t)}{\tau}; \quad F(t) = A_0 \sin\left(\omega t - \frac{\omega}{W}z\right) \tag{8}$$

where $y(t)$ is O_3 VMR, τ is the lifetime of the O_3, and $F(t)$ is the sinusoidal forcing with period of 20 or 8 months. The loss of O_3 is nonlinear so this is an approximate description. Define $\tan\phi = \omega\tau$, the solution to equation (8) is

$$y(t) = \left(y(0) - \frac{A_0 \sin(\omega z/W + \phi)}{\sqrt{1 + \omega^2\tau^2}}\right)e^{-t/\tau} - \frac{A_0 \sin\left(\omega t - \frac{\omega}{W}z - \phi\right)}{\sqrt{1 + \omega^2\tau^2}} \tag{9}$$

where $y(0)$ is the value of y at $t = 0$. Ignoring the first transient term, the sensitivity of the response of O_3 to the oscillatory forcing is

$$\alpha = \frac{\| y(t) \|}{\| F(t) \|} = \frac{1}{\sqrt{1 + \omega^2\tau^2}} \tag{10}$$

Because the lifetime of ozone is long in the lower stratosphere where most of the column resides, we have $\omega\tau \gg 1$ and $\alpha \approx \dfrac{1}{\omega\tau}$. Therefore the response of ozone to the QBO-AB is about $\dfrac{\omega_A + \omega_Q}{\omega_A - \omega_Q} \approx 2.5$ times larger than that of QBO-AB′.

3.2. Sensitivity Experiments A, B, and C

[22] To understand how the QBO-AB signal in column ozone, $C_{AQ}^{-} \exp[i(\omega_A - \omega_Q)t]$, is generated, we consider three possible mechanisms. First, the QBO-AB in the transport fields, $v_{AQ}^{-} \exp[i(\omega_A - \omega_Q)t]$, will produce a signal with a 20-month period in ozone. Second, the QBO and the annual cycle from the transport fields will interact to

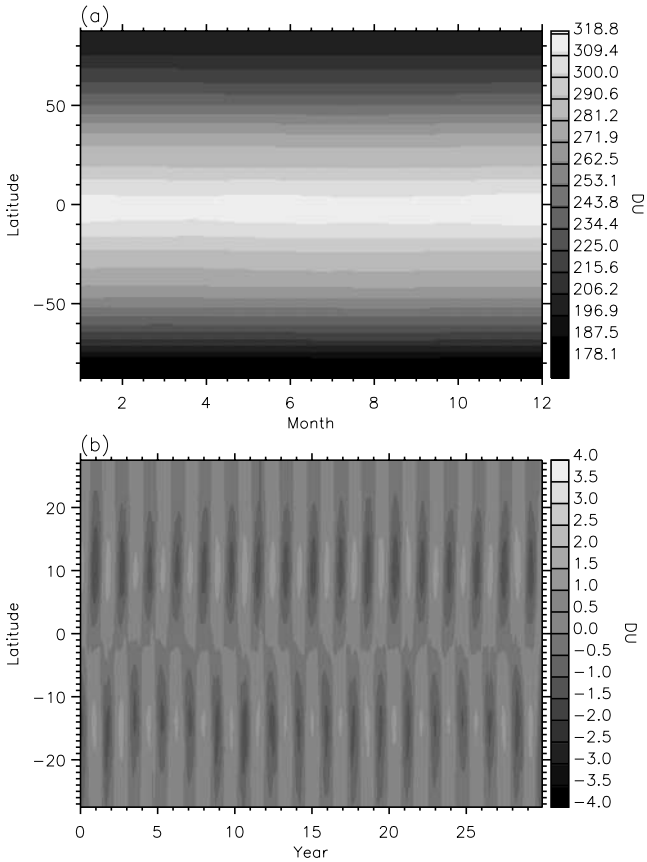

Figure 8. (a) Climatology and (b) anomaly of the total column ozone for experiment A. See color version of this figure at back of this issue.

produce a QBO-AB in the 2-D CTM. Finally, the interaction between the QBO in the transport and the annual cycle in the ozone chemistry will generate a QBO-AB. To determine the contributions of the three mechanisms in producing the QBO-AB signal in column ozone we have performed a series of sensitivity experiments.

[23] In experiment A, band-pass filter A is applied to the transport fields for extracting the QBO-AB signal, v_{AQ}^{-} exp $[i(\omega_A - \omega_Q)t]$. In this experiment we turn off the annual cycle in the photochemical production and loss rates (see equation (5)). As a result, shown in Figure 8a, there is no annual cycle in the total column ozone climatology from this 30-year model run. The ozone anomaly, shown in Figure 8b, displays a 20-month period characteristic of the QBO-AB. PCA is applied to the detrended and low-pass-filtered total column ozone anomaly. The first leading mode, shown in Figure 9, captures 97.4% of the total variance, representing the QBO-AB signal. This EOF is a tilted plane; values range from 1 DU in the north to −0.8 DU in the south. The magnitude is smaller than that of the second EOF in Figure 3d. The power spectral estimate of the associated PC has a dominant peak around 20 months, indicating that the ozone QBO-AB in this experiment is a direct result of the original QBO-AB signal in the transport fields. EEOF analysis is applied to the deseasonalized ozone VMR from experiment A. The first two modes, together accounting for 98% of the variance, correspond to the QBO-AB. We reconstruct the data using the first two EEOF modes. The 12.5°N $PC_1 \times EEOF_1 + PC_2 \times EEOF_2$ displays the upward propagation of the QBO-AB.

[24] In experiment B we retain the annual and QBO cycles in the transport fields by applying band-pass filters D and E. There is no annual cycle in the chemical terms. The climatology of the 30-year total column ozone and the ozone anomaly are shown in Figure 10. There is an annual cycle in the ozone, which is due to the annual cycle in the transport fields, v_A exp $(i\omega_A t)$. PCA is applied to the detrended, deseasonalized and filtered total column ozone anomaly. The first EOF represents the QBO. The second EOF, shown in Figure 11, captures 26.4% of the total variance and represents the QBO-AB signal. The values of this EOF range from 1 DU in the north to −1 DU in the south. The magnitude of this EOF is comparable to the first

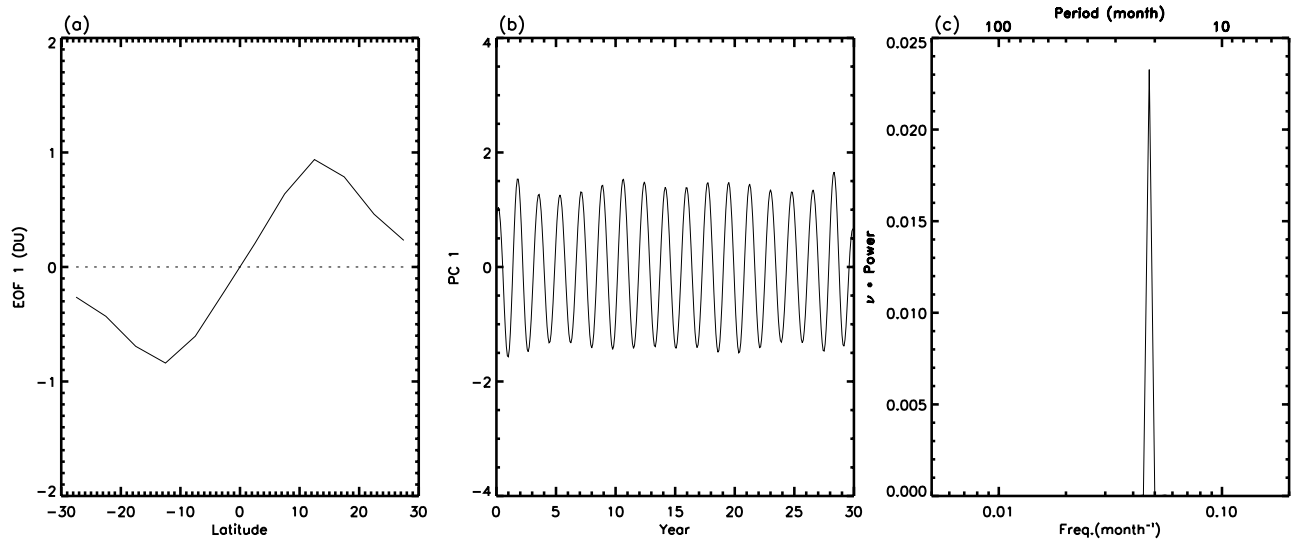

Figure 9. (a) Spatial EOF patterns, (b) PC time series, and (c) spectra for the first EOF of the total column ozone from experiment A. Units of EOFs are DU.

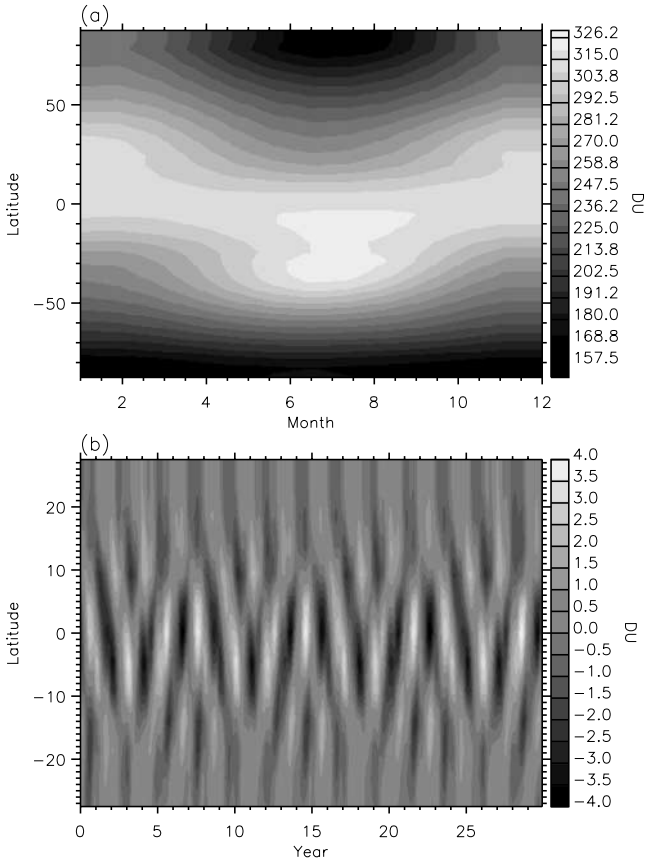

Figure 10. (a) Climatology and (b) anomaly of the total column ozone for experiment B. See color version of this figure at back of this issue.

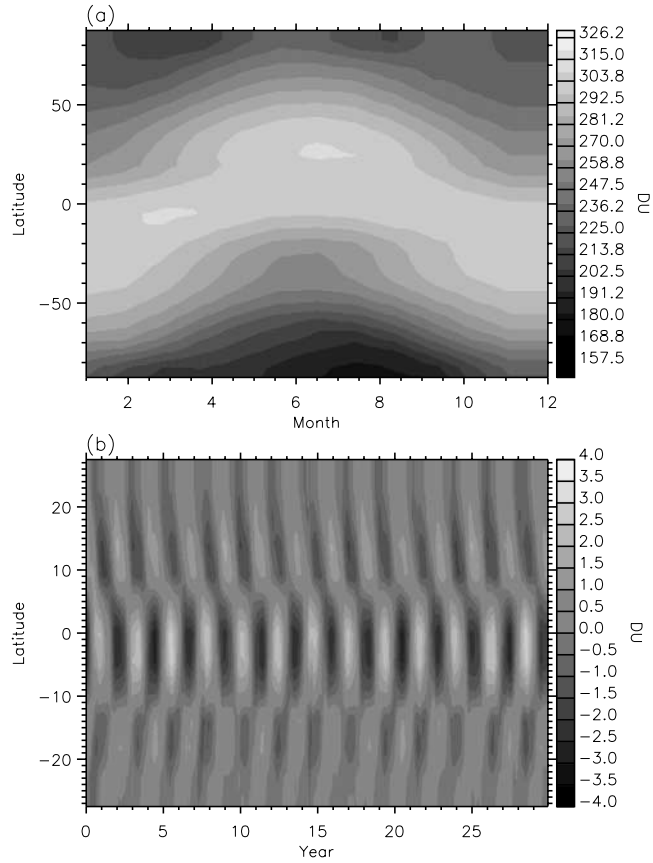

Figure 12. (a) Climatology and (b) anomaly of the total column ozone for experiment C. See color version of this figure at back of this issue.

EOF from experiment A. The ozone QBO-AB in this experiment is the result of the interaction between the QBO and annual signals from the transport fields in the 2-D CTM. EEOF is applied to the deseasonalized ozone VMR from experiment B. The third and fourth modes correspond to the QBO-AB, accounting for 14.2% and 13.3% of the variance, respectively. The $PC_3 \times EEOF_3 + PC_4 \times EEOF_4$ at 12.5°N also displays the upward propagation of the QBO-AB.

[25] Finally, we examine the interaction between the QBO and the annual cycle in the chemistry in experiment C by applying band-pass filter E to the transport fields to

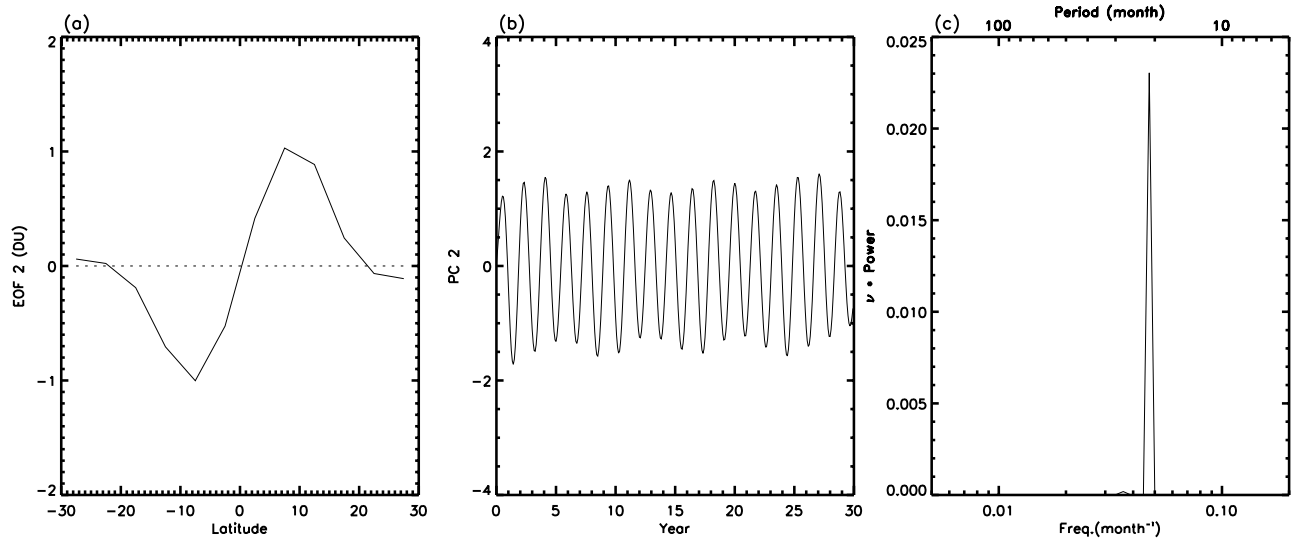

Figure 11. (a) Spatial EOF patterns, (b) PC time series, and (c) spectra for the first EOF of the total column ozone from experiment B. Units of EOFs are DU.

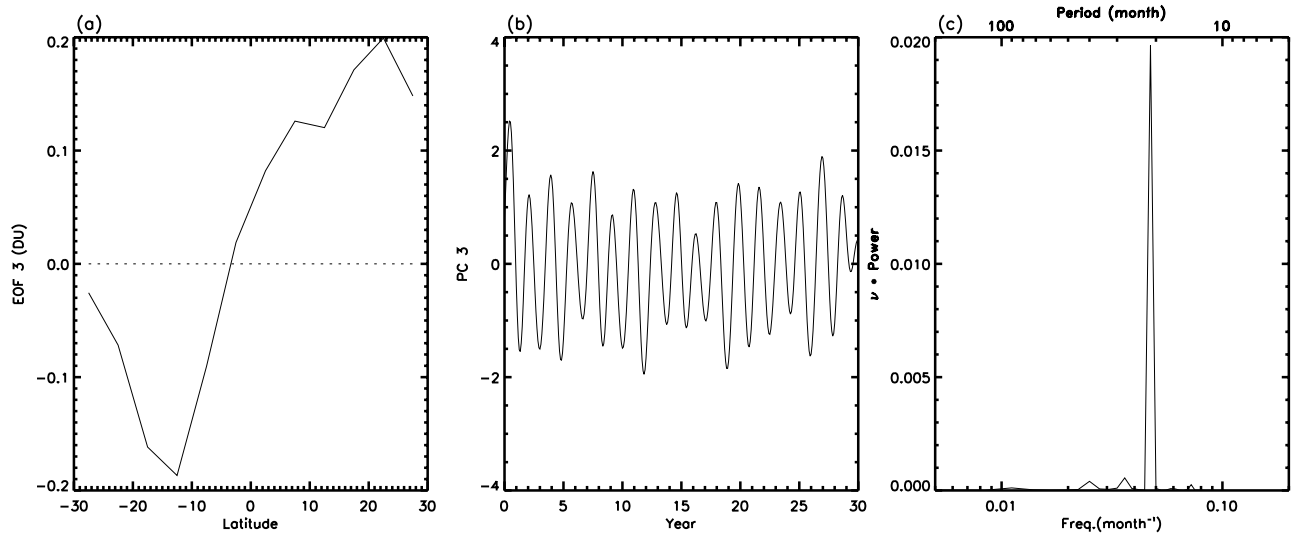

Figure 13. (a) Spatial EOF patterns, (b) PC time series, and (c) spectra for the first EOF of the total column ozone from experiment C. Units of EOFs are DU.

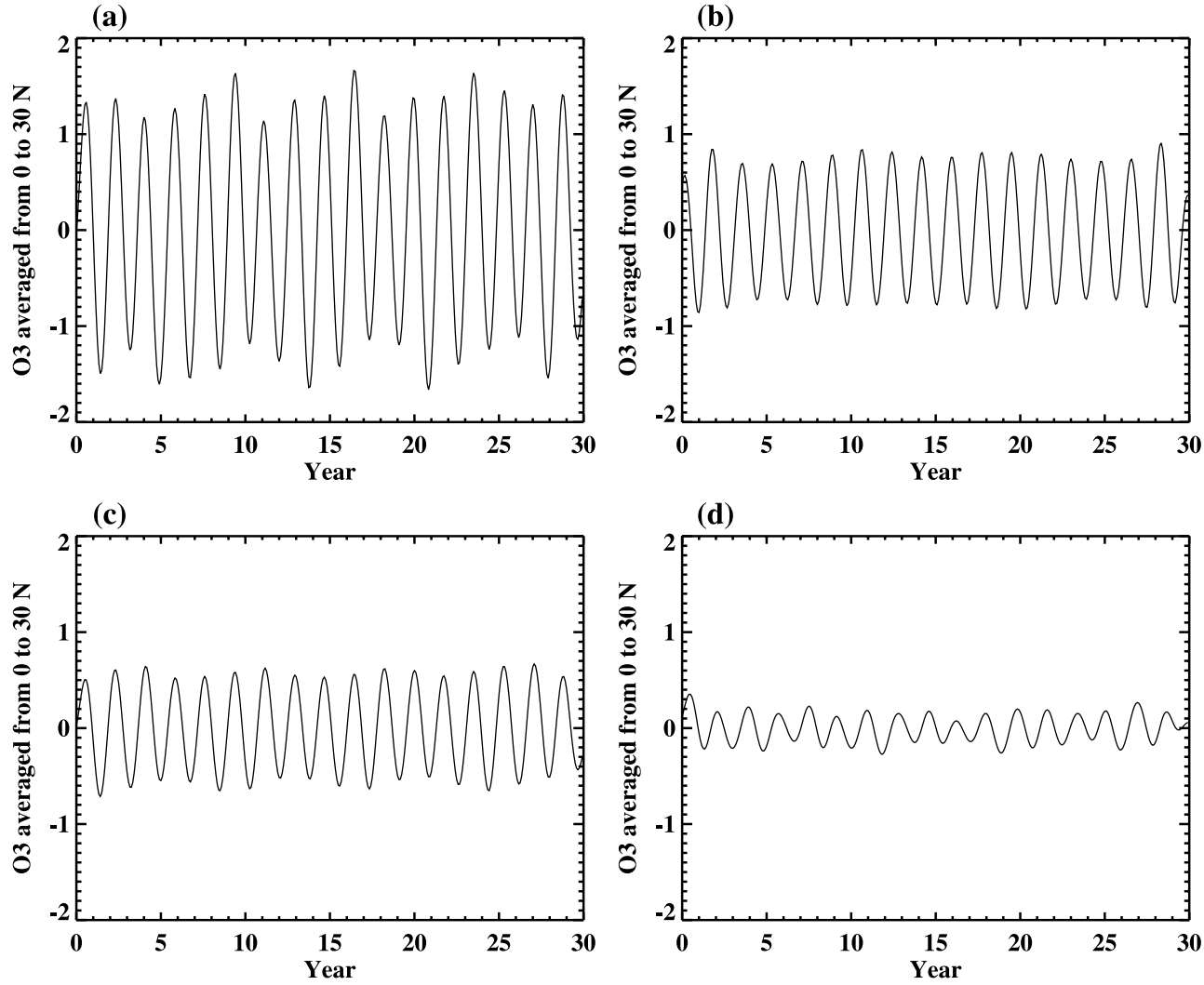

Figure 14. Product of the PC and EOF corresponding to the QBO-AB signal averaged from 0° to 30°N: (a) $PC_2 \times EOF_2$ of column ozone anomaly in the standard model, (b) $PC_1 \times EOF_1$ of column ozone anomaly in experiment A, (c) $PC_2 \times EOF_2$ of column ozone anomaly in experiment B, and (d) $PC_3 \times EOF_3$ of column ozone anomaly in experiment C. Units are DU.

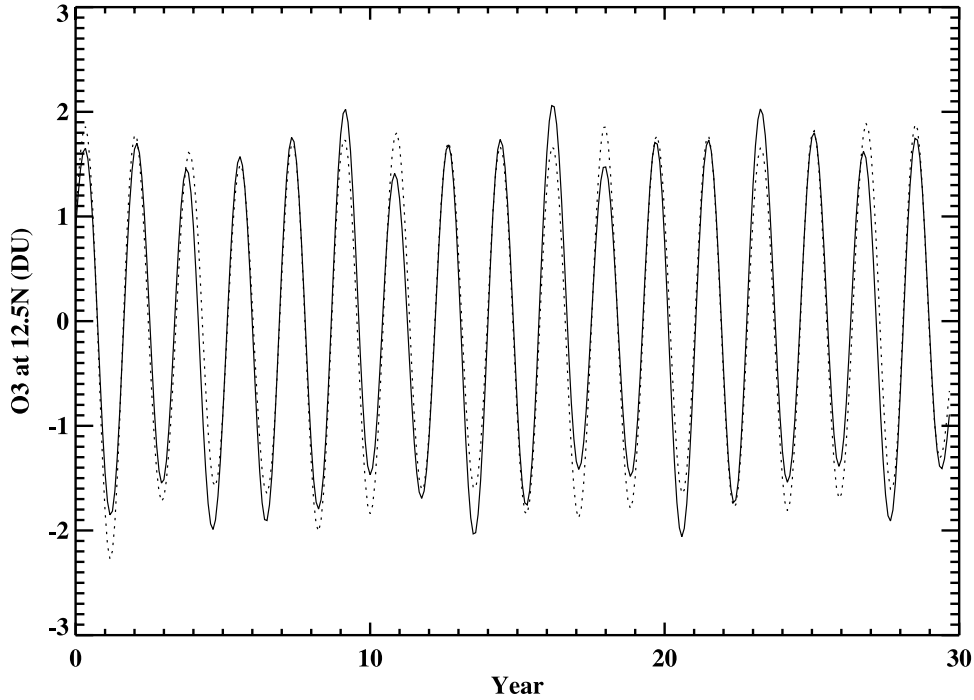

Figure 15. Comparison between the QBO-AB in the standard model (solid line) and the sum of the QBO-AB in experiments A, B, and C (dotted line). The QBO-AB signal is derived from the product of the PC and EOF corresponding to the QBO-AB. Units are DU.

retain only the QBO signal, $v_Q \exp(i\omega_Q t)$. The annual cycle is retained in the photochemical production and loss rates, $S_A \exp(i\omega_A t)$. As shown in Figure 12a, there is an annual cycle in the ozone climatology, which represents the change of photochemical production and loss rates by the annual march of solar heating. The ozone anomaly, shown in Figure 12b, has the QBO and QBO-AB signals. We applied PCA to the detrended, deseasonalized and filtered total column ozone anomaly. The first two EOFs correspond to the QBO. The third mode, shown in Figure 13, captures 2% of the total variance and represents the QBO-AB. Values of this EOF range from 0.2 DU in the north to −0.19 DU in the south, significantly smaller than that in experiments A and B. This suggests that the interaction between the QBO in the transport fields and the annual cycle in the chemistry model makes the smallest contribution to the ozone QBO-AB signal. The QBO-AB signal is too weak in ozone VMR from the experiment C, and does not appear in the leading EEOFs.

[26] To further investigate the magnitude of the QBO-AB signal in column ozone, we multiply the PC and EOF corresponding to the column ozone QBO-AB in each model experiment. Since the QBO-AB is an asymmetric mode, we average the product of the PC and EOF from 0° to 30°N. The results, shown in Figure 14, confirm that the magnitude of the ozone QBO-AB in experiments A and B is comparable. The ozone QBO-AB signal in experiment C is the smallest. We then summed the product of the PC and EOF corresponding to the QBO-AB signal at 12.5°N from all three experiments. In Figure 15, the sum (dotted line) is compared against the QBO-AB signal from the standard model shifted forward by 3 months (solid line). These two curves match well. The 3-month phase shift is mostly due to the Fourier filters applied to the original transport fields [*Tung and Yang*, 1994a].

4. Conclusions

[27] We have used an idealized 2-D CTM [*Jones et al.*, 1998] to study the spatial-temporal pattern of and the mechanisms responsible for producing QBO-AB in the stratospheric ozone. The model produces a QBO in the ozone with a period of 28 months. The amplitude of the modeled QBO anomalies of ozone in the tropics is about 7 DU, in agreement with observations [*Hasebe*, 1983; *Zawodny and McCormick*, 1991]. PCA was applied to the detrended, deseasonalized, and filtered total column ozone anomaly from the standard model. The first two EOFs capture over 98.5% of the total variance. The first EOF explains 70.3% of the variance, and is identified with the approximately symmetric QBO with a period of 28 months. The second EOF, capturing 28.2% of the variance, is the asymmetric QBO-AB with a period of 20 months, arising from the interaction between the QBO and the annual cycle. EEOF analysis of the deseasonalized model ozone VMR illustrates that the ozone QBO and QBO-AB are vertical propagating features. The QBO propagates downward, in agreement with previous analysis. However, the QBO-AB propagates upward as a result of the interaction between the BDC and QBO. We also found similar propagations of the ozone QBO and QBO-AB in the MOD.

[28] Sensitivity experiments were performed to isolate the mechanism primarily responsible for the QBO-AB signal in total column ozone. Our analysis indicate that the interaction between the QBO signal in the transport fields and the annual cycle in the chemistry play a minor role in generating

the QBO-AB in ozone in the model. We found that the dynamical QBO-AB in the MMC and the interaction between the QBO and the annual cycle in the transport fields provide comparable contributions to the QBO-AB in ozone. The idealized model employed here is not able to match the observed QBO phase. In future work we will investigate the details of the phase relationship between the ozone anomalies and the QBO in zonal wind by relaxing the model zonal winds to match observed tropical winds, to reproduce the interannual variability of the QBO in the model. Extension of the model to higher latitudes is also being planned.

[29] This work constitutes an advance beyond the work of *Camp et al.* [2003] and *Jiang et al.* [2004] in elucidating the nonlinear interaction between the QBO and the annual cycle, primarily the BDC. It is a tribute to the high quality of the MOD data that we can now extract a second-order signal that is less than 1% of the bulk signal. This allows us to sensitively probe nonlinear interactions between the different physical processes in the atmosphere. It is desirable to extend our data analysis and modeling to investigate related nonlinear interactions such as that between QBO and the solar cycle [*Labitzke and Vanloon*, 1988; *Hamilton*, 2002; *Salby and Callaghan*, 2000]. Longer records and improvements in measurements will provide the necessary data to test critical components of our model.

[30] **Acknowledgments.** We thank A. Ruzmaikin, J. Feynman, V. Natraj, and M. Gerstell for their helpful comments. This work was supported in part by NASA grants NAG1-1806 and NNG04GN02G to the California Institute of Technology. The fourth author was supported by the Human Resources Development Fund at the Jet Propulsion Laboratory.

References

Angell, J. K., and J. Korshover (1970), Quasi-biennial, annual, and semi-annual zonal wind and temperature harmonic amplitudes and phases in stratosphere and low mesosphere of Northern Hemisphere, *J. Geophys. Res.*, *75*(3), 543–550.

Baldwin, M. P., and K. K. Tung (1994), Extra-tropical QBO signals in angular-momentum and wave forcing, *Geophys. Res. Lett.*, *21*(24), 2717–2720.

Baldwin, M. P., et al. (2001), The quasi-biennial oscillation, *Rev. Geophys.*, *39*(2), 179–229.

Camp, C. D., M. S. Roulston, A. F. C. Haldemann, and Y. L. Yung (2001), The sensitivity of tropospheric methane to the interannual variability in stratospheric ozone, *Chemosphere Global Change Sci.*, *3*, 147–156.

Camp, C. D., M. S. Roulston, and Y. L. Yung (2003), Temporal and spatial patterns of the interannual variability of total ozone in the tropics, *J. Geophys. Res.*, *108*(D20), 4643, doi:10.1029/2001JD001504.

Dunkerton, T. J., and M. P. Baldwin (1991), Quasi-biennial modulation of planetary-wave fluxes in the Northern-Hemisphere winter, *J. Atmos. Sci.*, *48*(8), 1043–1061.

Gray, L. J., and T. J. Dunkerton (1990), The role of the annual cycle in the quasi-biennial oscillation of ozone, *J. Atmos. Sci.*, *47*(20), 2429–2451.

Gray, L. J., and J. A. Pyle (1989), A two-dimensional model of the quasi-biennial oscillation of ozone, *J. Atmos. Sci.*, *46*(2), 203–220.

Hamilton, K. (2002), On the quasi-decadal modulation of the stratospheric QBO period, *J. Clim.*, *15*(17), 2562–2565.

Hasebe, F. (1983), Interannual variations of global total ozone revealed from Nimbus 4-BUV and ground-based observations, *J. Geophys. Res.*, *88*(C11), 6819–6834.

Hasebe, F. (1994), Quasi-biennial oscillations of ozone and diabatic circulation in the equatorial stratosphere, *J. Atmos. Sci.*, *51*(5), 729–745.

Holton, J. R., and R. S. Lindzen (1972), Updated theory for quasi-biennial cycle of tropical stratosphere, *J. Atmos. Sci.*, *29*(6), 1076–1080.

Holton, J. R., and H. C. Tan (1980), The influence of the equatorial quasi-biennial oscillation on the global circulation at 50 mb, *J. Atmos. Sci.*, *37*(10), 2200–2208.

Jiang, X., C. D. Camp, R. Shia, D. Noone, C. Walker, and Y. L. Yung (2004), Quasi-biennial oscillation and quasi-biennial oscillation–annual beat in the tropical total column ozone: A two-dimensional model simulation, *J. Geophys. Res.*, *109*, D16305, doi:10.1029/2003JD004377.

Jones, D. B. A. (1998), An analysis of the mechanisms for the QBO in ozone in the tropical and subtropical stratosphere, Ph. D. thesis, Harvard Univ., Cambridge, Mass.

Jones, D. B. A., H. R. Schneider, and M. B. McElroy (1998), Effects of the quasi-biennial oscillation on the zonally averaged transport of tracers, *J. Geophys. Res.*, *103*(D10), 11,235–11,249.

Kinnersley, J. S., and K. K. Tung (1999), Mechanisms for the extratropical QBO in circulation and ozone, *J. Atmos. Sci.*, *56*(12), 1942–1962.

Labitzke, K., and H. Vanloon (1988), Associations between the 11-year solar-cycle, the QBO and the atmosphere 1. The troposphere and stratosphere in the Northern Hemisphere in winter, *J. Atmos. Terr. Phys.*, *50*(3), 197–206.

Newman, P. A., M. R. Schoeberl, and R. A. Plumb (1986), Horizontal mixing coefficients for two-dimensional chemical models calculated from National Meteorological Center data, *J. Geophys. Res.*, *91*(D7), 7919–7924.

Newman, P. A., M. R. Schoeberl, R. A. Plumb, and J. E. Rosenfield (1988), Mixing rates calculated from potential vorticity, *J. Geophys. Res.*, *93*(D5), 5221–5240.

Oltmans, S. J., and J. London (1982), The quasi-biennial oscillation in atmospheric ozone, *J. Geophys. Res.*, *87*(C11), 8981–8989.

Pawson, S., and M. Fiorino (1998), A comparison of reanalyses in the tropical stratosphere. Part 2: The quasi-biennial oscillation, *Clim. Dyn.*, *14*(9), 645–658.

Plumb, R. A., and R. C. Bell (1982), A model of the quasi-biennial oscillation on an equatorial beta-plane, *Q. J. R. Meteorol. Soc.*, *108*(456), 335–352.

Politowicz, P. A., and M. H. Hitchman (1997), Exploring the effects of forcing quasi-biennial oscillations in a two-dimensional model, *J. Geophys. Res.*, *102*(D14), 16,481–16,497.

Randel, W. J., and J. B. Cobb (1994), Coherent variations of monthly mean total ozone and lower stratospheric temperature, *J. Geophys. Res.*, *99*, 5433–5447.

Randel, W. J., and F. Wu (1996), Isolation of the ozone QBO in SAGE II data by singular-value decomposition, *J. Atmos. Sci.*, *53*(17), 2546–2559.

Randel, W. J., F. Wu, R. Swinbank, J. Nash, and A. O'Neill (1999), Global QBO circulation derived from UKMO stratospheric analyses, *J. Atmos. Sci.*, *56*(4), 457–474.

Reed, R. J., W. J. Campbell, L. A. Rasmussen, and D. G. Rogers (1961), Evidence of a downward-propagating, annual wind reversal in the equatorial stratosphere, *J. Geophys. Res.*, *66*(3), 813–818.

Ruzmaikin, A., J. Feynman, X. Jiang, and Y. L. Yung (2005), Extratropical signature of the quasi-biennial oscillation, *J. Geophys. Res.*, *110*, D11111, doi:10.1029/2004JD005382.

Salby, M., and P. Callaghan (2000), Connection between the solar cycle and the QBO: The missing link, *J. Clim.*, *13*(14), 2652–2662.

Schneider, H. R., D. B. A. Jones, M. B. McElroy, and G. Y. Shi (2000), Analysis of residual mean transport in the stratosphere: 1. Model description and comparison with satellite data, *J. Geophys. Res.*, *105*(D15), 19,991–20,011.

Tung, K. K., and H. Yang (1994a), Global QBO in circulation and ozone: 1. Reexamination of observational evidence, *J. Atmos. Sci.*, *51*(19), 2699–2707.

Tung, K. K., and H. Yang (1994b), Global QBO in circulation and ozone: 2. A simple mechanistic model, *J. Atmos. Sci.*, *51*(22), 3365.

Veryard, R. G., and R. A. Ebdon (1961), Fluctuations in tropical stratospheric winds, *Meteorol. Mag.*, *90*, 125–143.

Waliser, D. E., K. M. Lau, W. Stern, and C. Jones (2003), Potential predictability of the Madden-Julian oscillation, *Bull. Am. Meteorol. Soc.*, *84*(1), 33–50.

Weare, B. C., and J. S. Nasstrom (1982), Examples of extended empirical orthogonal function analyses, *Mon. Weather Rev.*, *110*(6), 481–485.

Wellemeyer, C., P. K. Bhartia, S. Taylor, W. Qin, and C. Ahn (2004), Version 8 Total Ozone Mapping Spectrometer (TOMS) algorithm, in *Proceedings of the XX Quadrennial Ozone Symposium*, edited by C. Zerefos, pp. 635–636, Int. Ozone Comm., Athens.

Zawodny, J. M., and M. P. McCormick (1991), Stratospheric Aerosol and Gas Experiment II measurements of the quasi-biennial oscillations in ozone and nitrogen dioxide, *J. Geophys. Res.*, *96*(D5), 9371–9377.

X. Jiang, Department of Environmental Science and Engineering, California Institute of Technology, MS 150-21, Pasadena, CA 91125, USA. (xun@gps.caltech.edu)

D. B. A. Jones, Department of Physics, University of Toronto, 60 St. George Street, Toronto, Ontario, Canada M5S 1A7.

R. Shia and Y. L. Yung, Division of Geological and Planetary Sciences, California Institute of Technology, MS 150-21, Pasadena, CA 91125, USA.

D. E. Waliser, Sciences Division, Jet Propulsion Laboratory, MS 183-501, California Institute of Technology, Pasadena, CA 91109, USA.

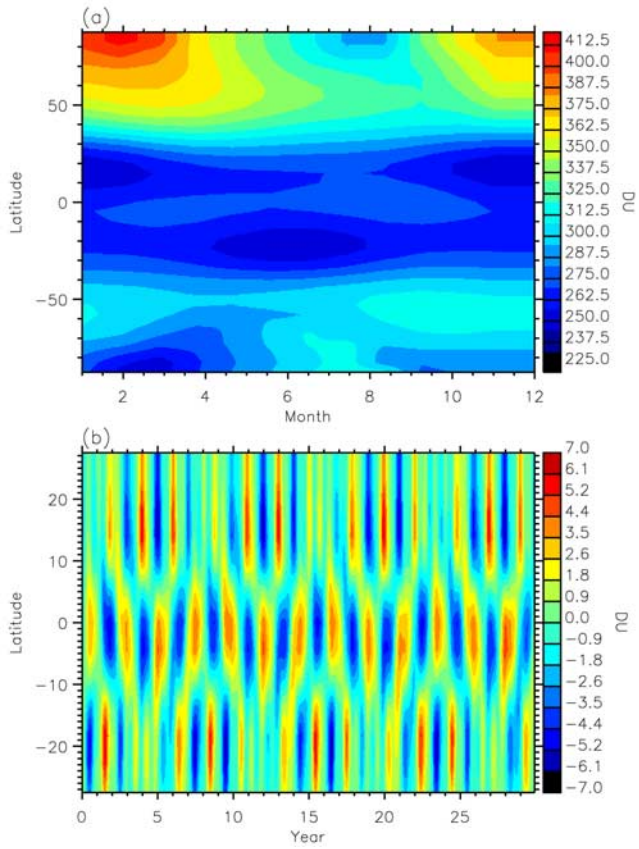

Figure 1. (a) Climatology and (b) anomaly of the total column ozone for the standard model.

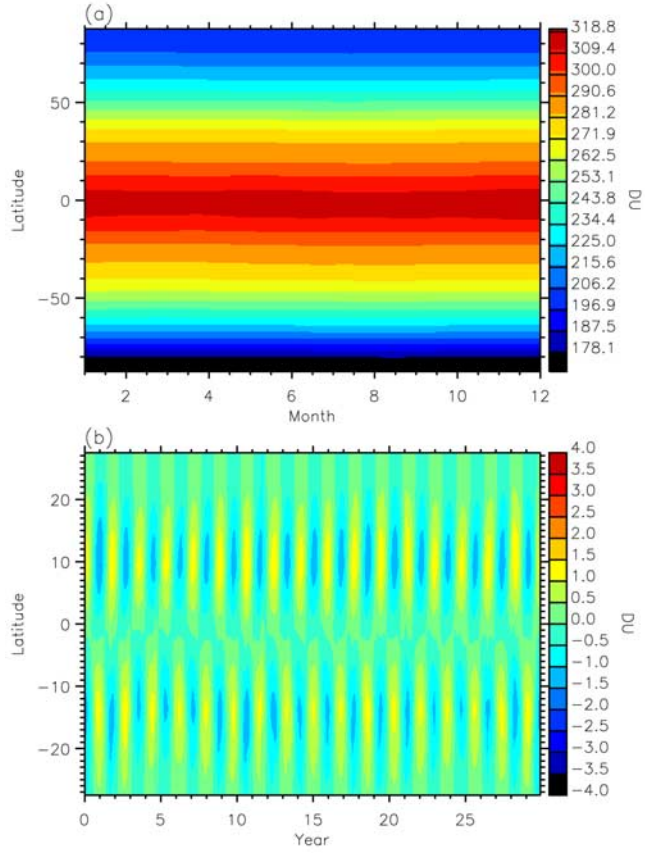

Figure 8. (a) Climatology and (b) anomaly of the total column ozone for experiment A.

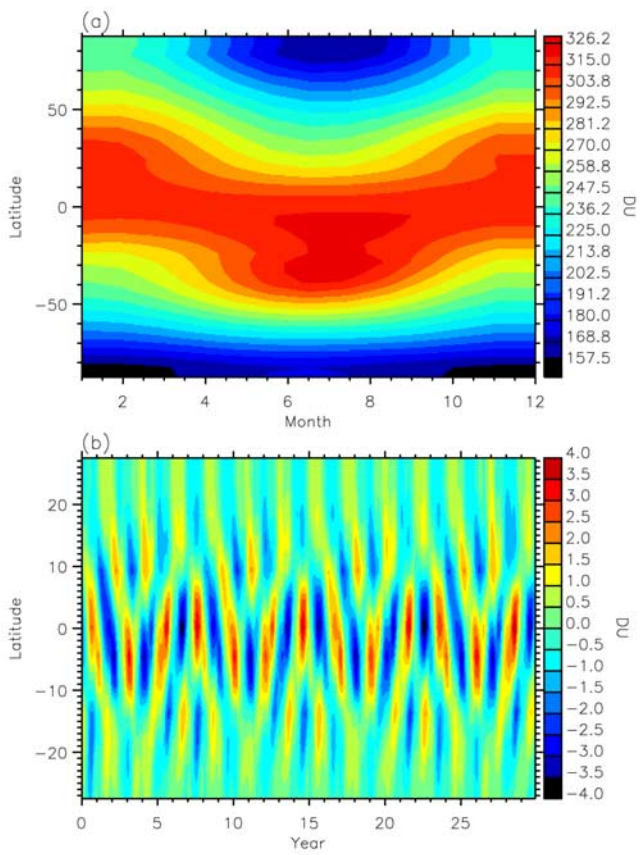

Figure 10. (a) Climatology and (b) anomaly of the total column ozone for experiment B.

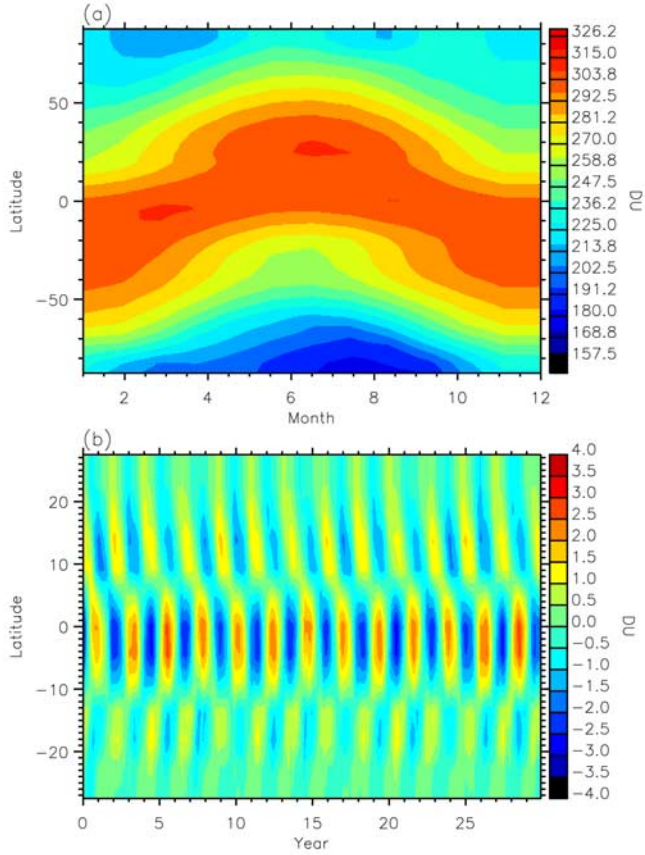

Figure 12. (a) Climatology and (b) anomaly of the total column ozone for experiment C.